Electronic Supplementary Material (ESI) for Dalton Transactions.
This journal is © The Royal Society of Chemistry 2020

Supporting Information

High stability and luminance efficiency thieno[2,3-*d*]pyridazine-based iridium complexes and their application in high-performance yellow OLEDs

Qunying Mei,[a†] Ren Sheng,[†b] Wei Cheng,[†a] Jie Zhang,[a] Ping Wang,[a] Qunbo Mei,*[c] Ping Chen,*[b] and Bihai Tong*[a]

[a]Key Laboratory of Metallurgical Emission Reduction & Resources Recycling, Ministry of Education, Institute of Molecular Engineering and Applied Chemistry, School of Metallurgy Engineering, Anhui University of Technology, Maanshan, 243002, Anhui, China. E-mail: tongbihai@163.com

[b]State Key Laboratory on Integrated Optoelectronics, College of Electronic Science and Engineering, Jilin University, Changchun 130012, P. R. China. E-mail: pingchen@jlu.edu.cn

[c] Key Laboratory for Organic Electronics and Information Displays & Institute of Advanced Materials (IAM), Jiangsu National Synergetic Innovation Center for Advanced Materials (SICAM), Nanjing University of Posts & Telecommunications, Nanjing, 210023, Jiangsu, China. E-mail: iamqbmei@njupt.edu.cn

[†] These authors contributed equally to this work.

* Corresponding authors.

Contents:

1. General descriptions
2. **Fig. S1** The emission decay curves ((a) in degassed and aerated CH_2Cl_2; (b) in PMMA films at a conc. of 1 wt%) and (c) PL spectra (at RT and 77K) of new iridium complex in PMMA films.
3. **Table S1** Supplementary physical properties for the iridium complexes.
4. ^{1}H- and ^{19}F-NMR spectra of all new compounds.
5. High resolution mass spectrometers (HRMS) of all new compounds.
6. References

1. General descriptions

1.1. Materials and characterization

All the materials and solvents were obtained commercially and used as received without further purification. Proton NMR spectra were measured on a Bruker AV400 spectrometer. High resolution mass spectra (HRMS) were recorded with a TOF 5600^{plus} mass spectrometer. X-ray crystallography diffraction was carried out on a Bruker SMART Apex CCD diffractometer. Cyclic voltammetry (CV) was measured on a CHI1140B Electrochemical Analyzer through a three-electrode system with a glassy carbon disk as the working electrode, platinum plate as the counter electrode and Ag/AgCl as the reference electrode. UV/Vis absorption spectra were recorded on a Purkinje General TU-1901 spectrophotometer. The PL spectra were recorded on a PerkinElmer LS-55 fluorescence spectrophotometer. The PL quantum efficiency and lifetime were measured with an Edinburgh FLS980 instrument.

1.2. Computational methodology

B3LYP functional was used to optimize the geometrical structures of ground state (S_0).[1] A "double-ξ" quality basis set consisting of Hay and Wadt's effective core potentials (ECP), LANL2DZ,[2] was employed to the Ir atom. 6-31G(d) basis set[3] was applied to other nonmetallic atoms. The solvent effect in CH_2Cl_2 medium was considered throughout the calculations. Combined with VMD program,[5] the molecular orbital was visualized by Multiwfn code.[4] The frontier molecular orbital (FMO) distribution in molecules was analyzed by Multiwfn using Mulliken population analysis. Gaussian 16 software package was used for calculations.[6]

1.3. OLED fabrication

The OLEDs were grown on pre-patterned ITO coated glass (≈ 20 Ω square^{-1}). Before depositing into the evaporation system, the ITO substrates were cleaned with acetone, ethyl alcohol, and deionized water by ultrasonic cleaning machine for 20 min. All the devices were deposited sequentially under fine vacuum of 8×10^{-5} Pa. The organic transport materials were grown by the rate of 0.08-0.15 nm s^{-1}, while organic dopants, AlQ_3 were deposited at the rate of 0.02-0.15 Å s^{-1},

Al was deposited by the rate of 3 Å s^{-1}. The CIE coordinates, luminance, and EL spectra were carried out by a PR655 spectra-scan photometer simultaneously. The current density-voltage characteristics were tested by a programmable Keithley source-measure 2400 and PR655 spectra-scan.

2.

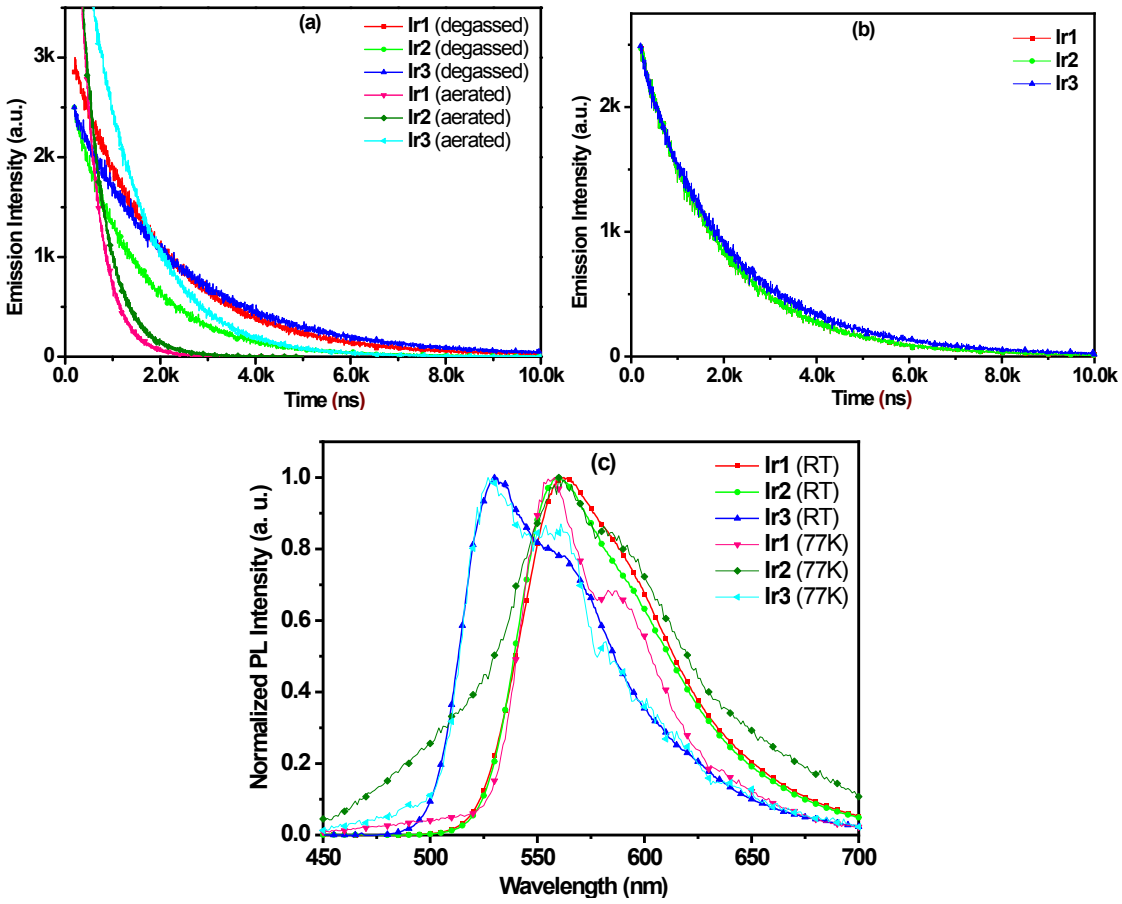

Fig. S1 The emission decay curves ((a) in degassed and aerated CH_2Cl_2; (b) in PMMA films at a conc. of 1 wt%) and (c) PL spectra (at RT and 77K) of new iridium complex in PMMA films.

3.

Table S1 Supplementary physical properties for the iridium complexes.

Sample	λ_{abs}[a] (nm)	λ_{em} (FWHM)[a] (nm)	λ_{em}(FWHM)[b] (nm)	k_r[c] ($\times 10^5$ s^{-1})	k_{nr}[c] ($\times 10^5$ s^{-1})
Ir1	256, 303, 383, 480	564(78)	563(74)	3.97 [3.17, 5.12]	1.46 [21.22, 0.69]
Ir2	261, 307, 361, 480	563(70)	561(73)	6.54 [4.20, 5.73]	0.81 [15.80, 0.12]
Ir3	310, 350, 414	534(77)	531(73)	2.98 [3.10, 4.87]	1.61 [5.52, 0.37]

[a] UV-Vis and photoluminescence spectra were recorded in CH_2Cl_2 at a conc. of 10^{-5} M. FWHM = full width at half maxima. [b] Photoluminescence spectra were recorded in PMMA at a conc. of 1 wt%. [c] The radiative/ irradiative decay rate constants (k_r/k_{nr}) of new iridium complexes in degassed CH_2Cl_2

[aerated CH_2Cl_2, PMMA films at a conc. of 1 wt%] at RT, which are calculated by $k_r = \Phi/\tau_{obs}$ and $k_{nr} = 1/\tau_{obs} - k_r$.

4. ^{1}H- and ^{19}F-NMR spectra of all new compounds.

^{1}H-NMR Spectrum of **btptpH** in C*D*Cl_3 (400 MHz):

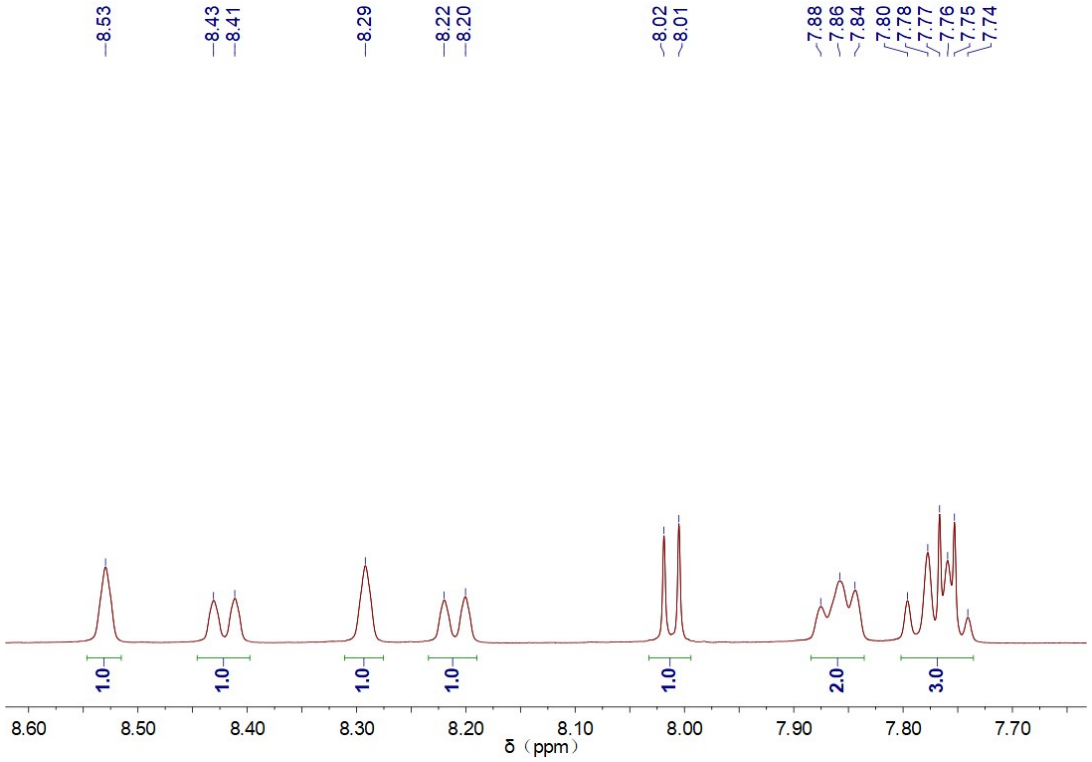

^{19}F-NMR Spectrum of **btptpH** in C*D*Cl_3 (376 MHz):

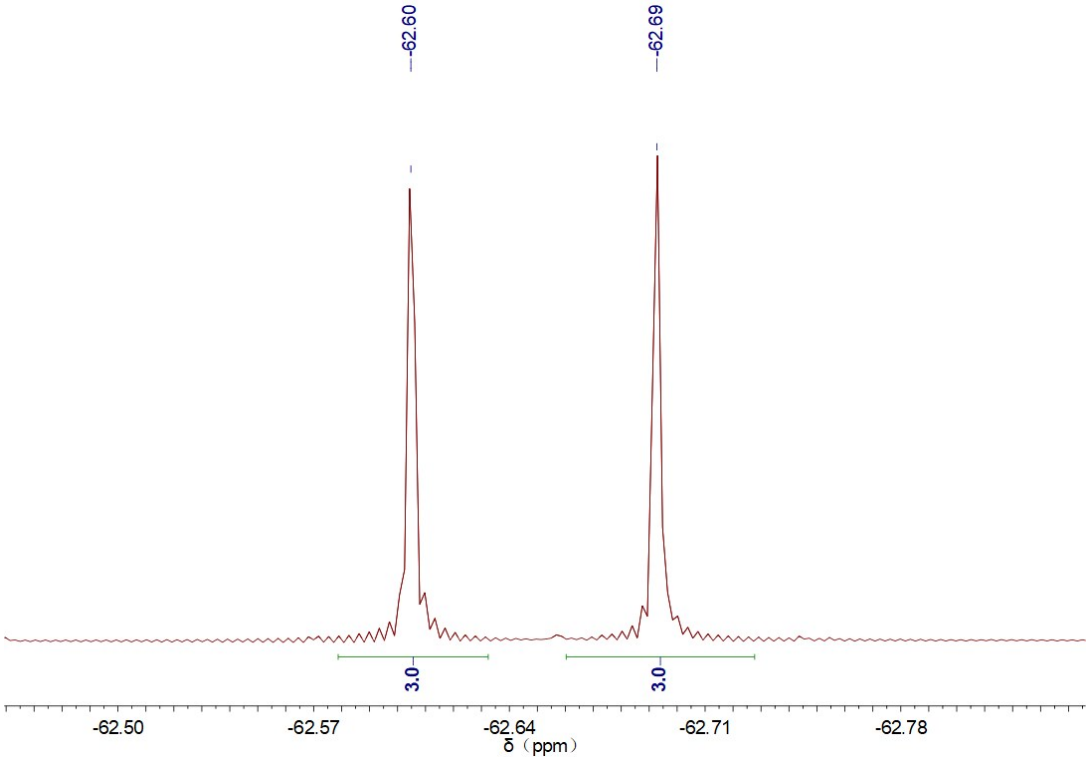

^{1}H-NMR Spectrum of **Ir1** in C*D*Cl$_3$ (400 MHz):

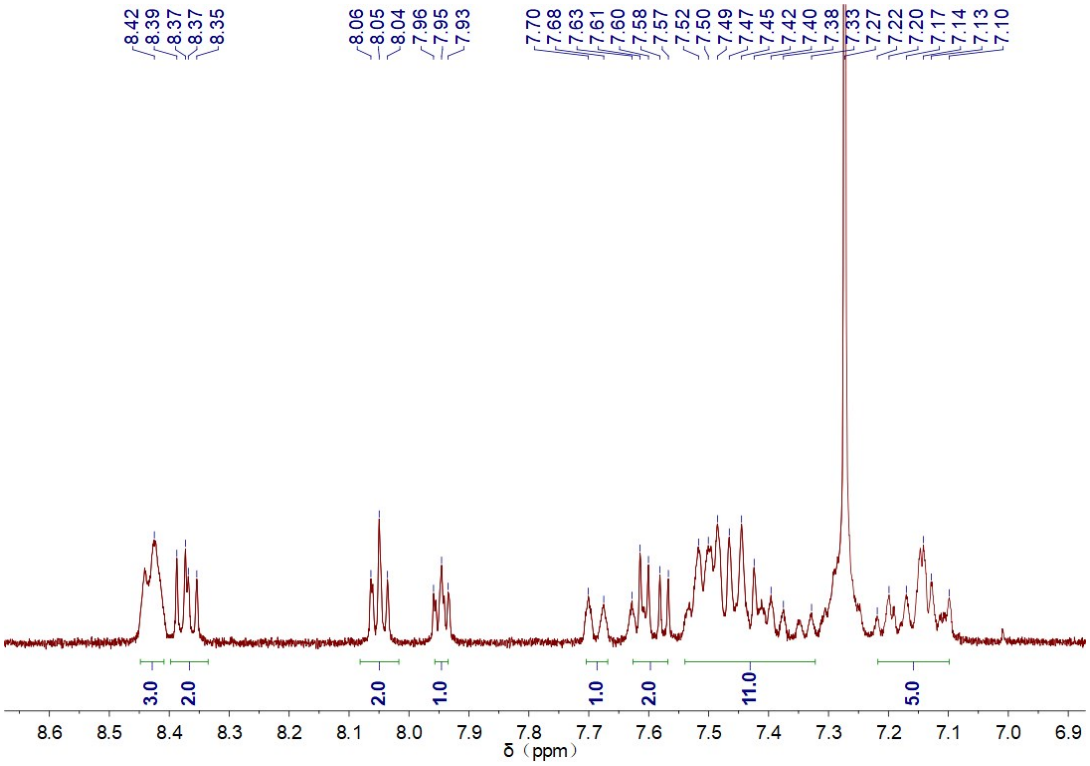

^{19}F-NMR Spectrum of **Ir1** in C*D*Cl$_3$ (376 MHz):

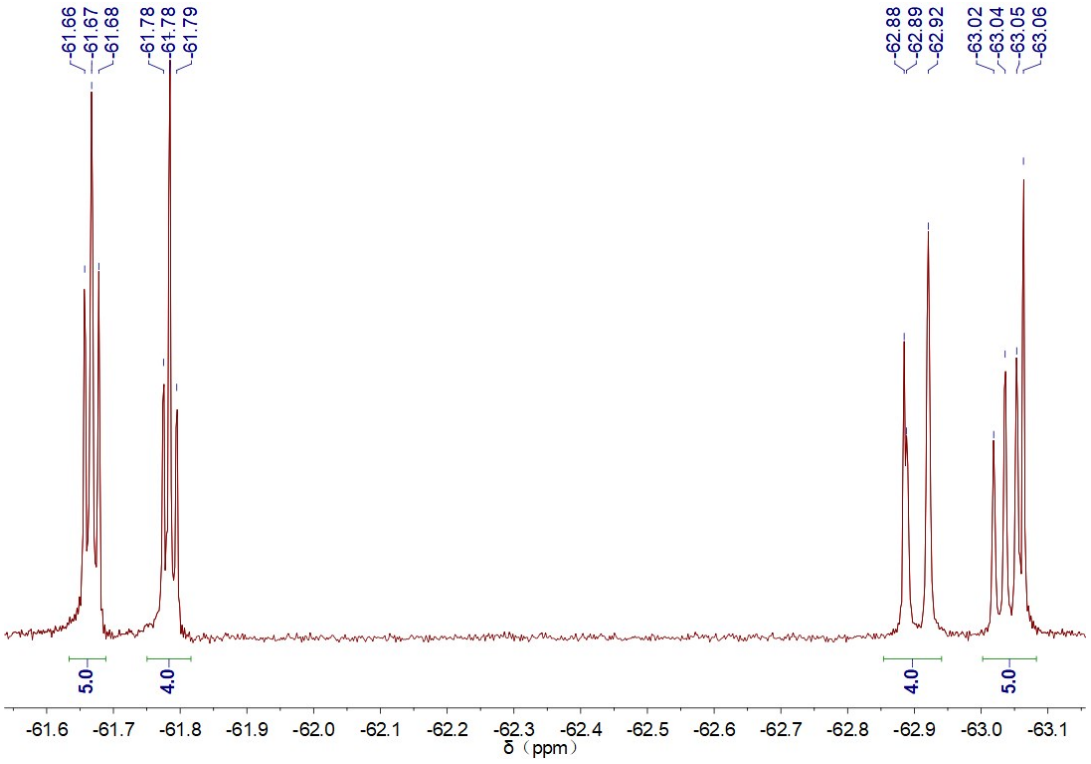

^{1}H-NMR Spectrum of **Ir2** in C*D*Cl$_3$ (400 MHz):

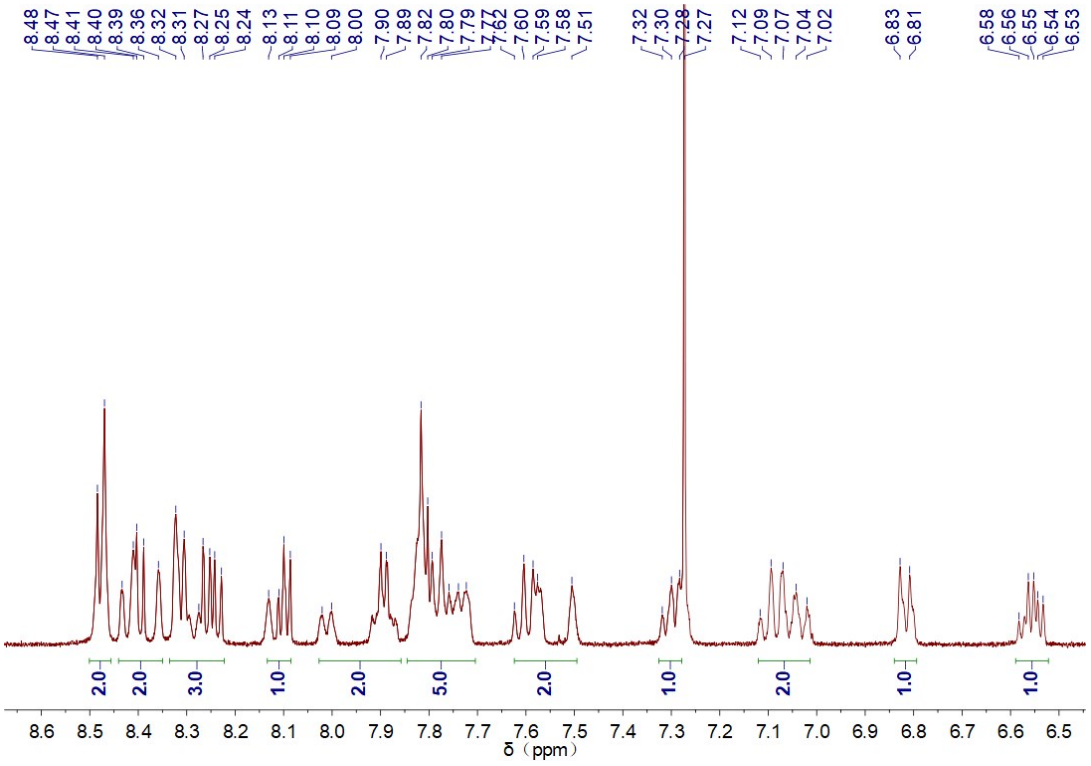

^{19}F-NMR Spectrum of **Ir2** in C*D*Cl$_3$ (376 MHz):

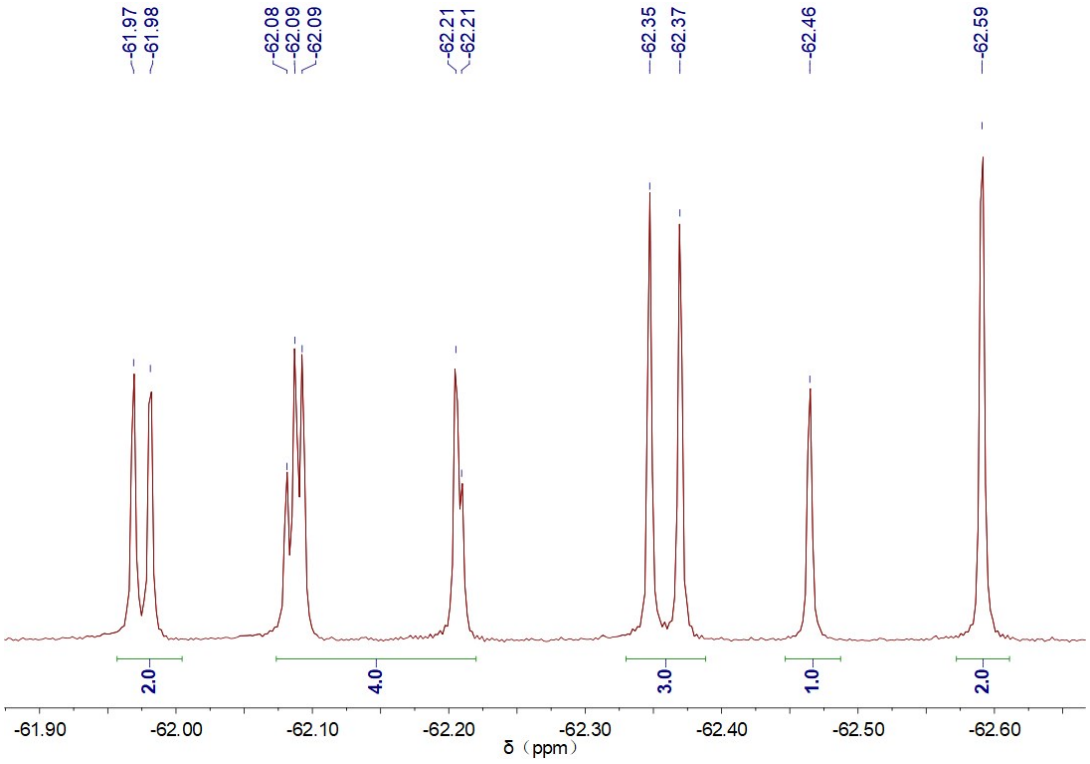

^{1}H-NMR Spectrum of **qtptpH** in C*D*Cl$_3$ (400 MHz):

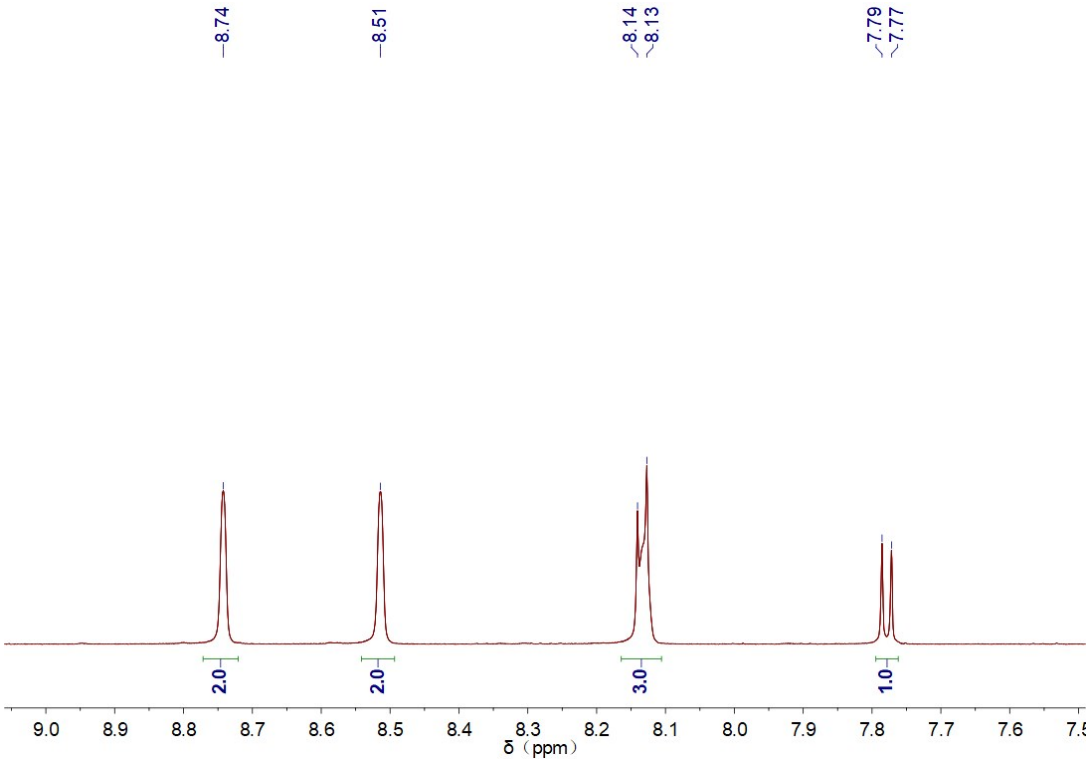

^{19}F-NMR Spectrum of **qtptpH** in C*D*Cl$_3$ (376 MHz):

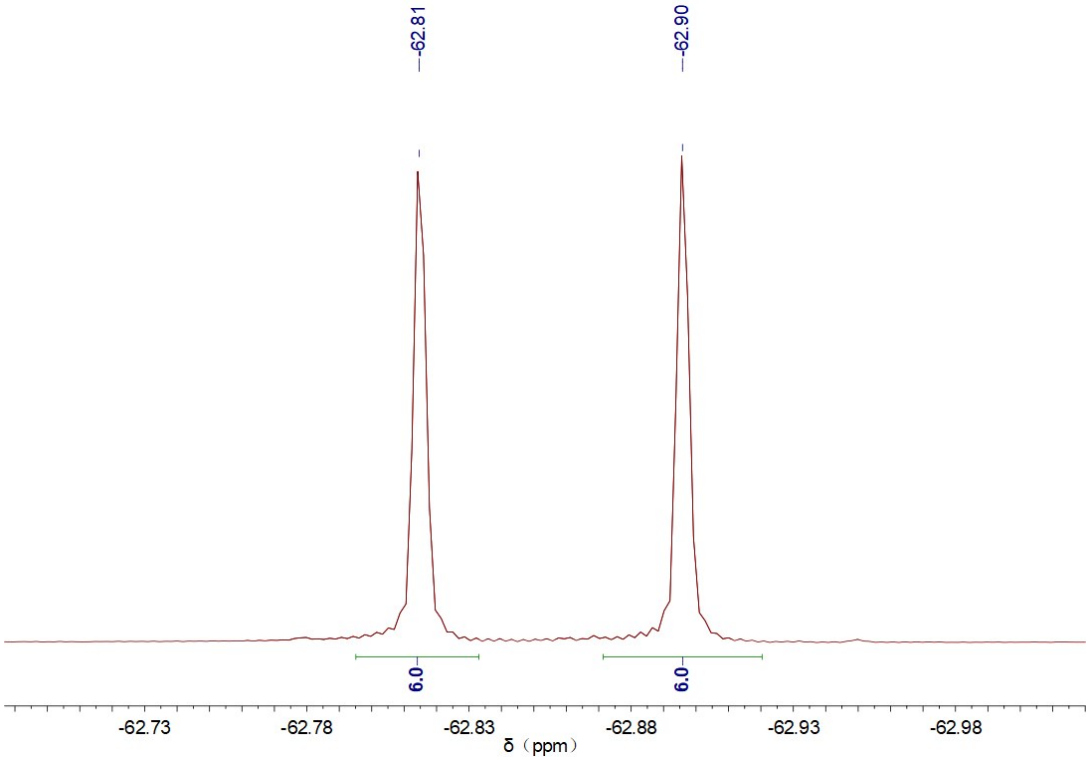

^{1}H-NMR Spectrum of **Ir3** in C*D*Cl$_3$ (400 MHz):

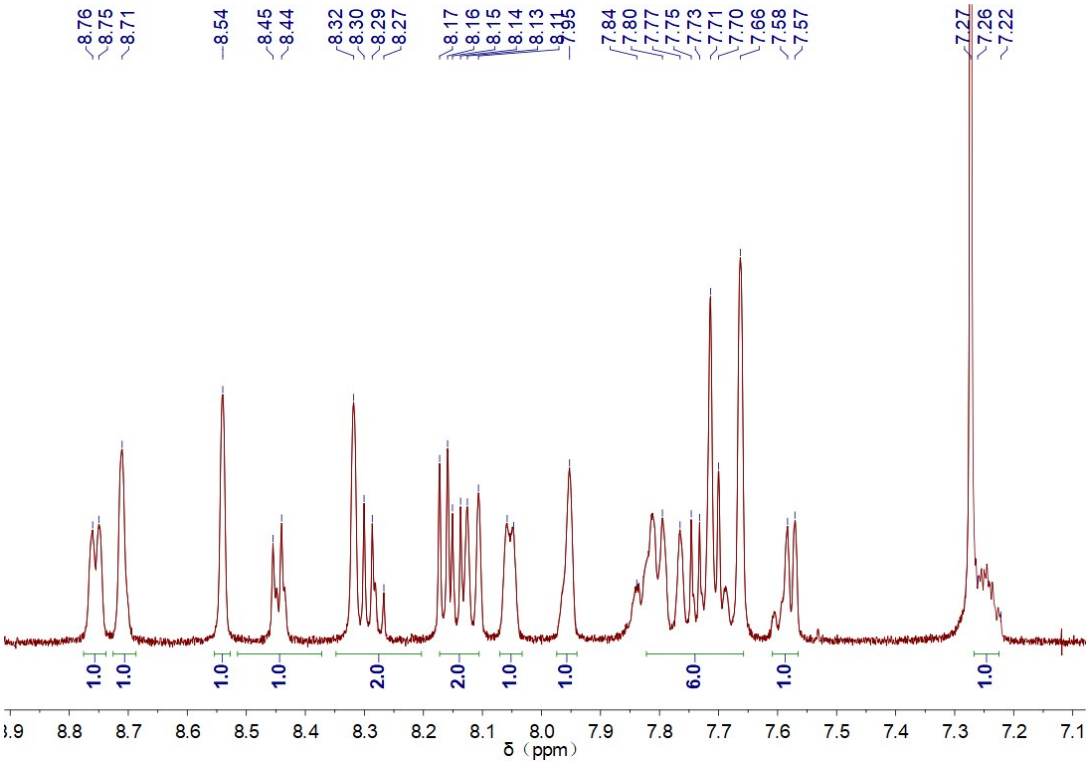

^{19}F-NMR Spectrum of **Ir3** in C*D*Cl$_3$ (376 MHz):

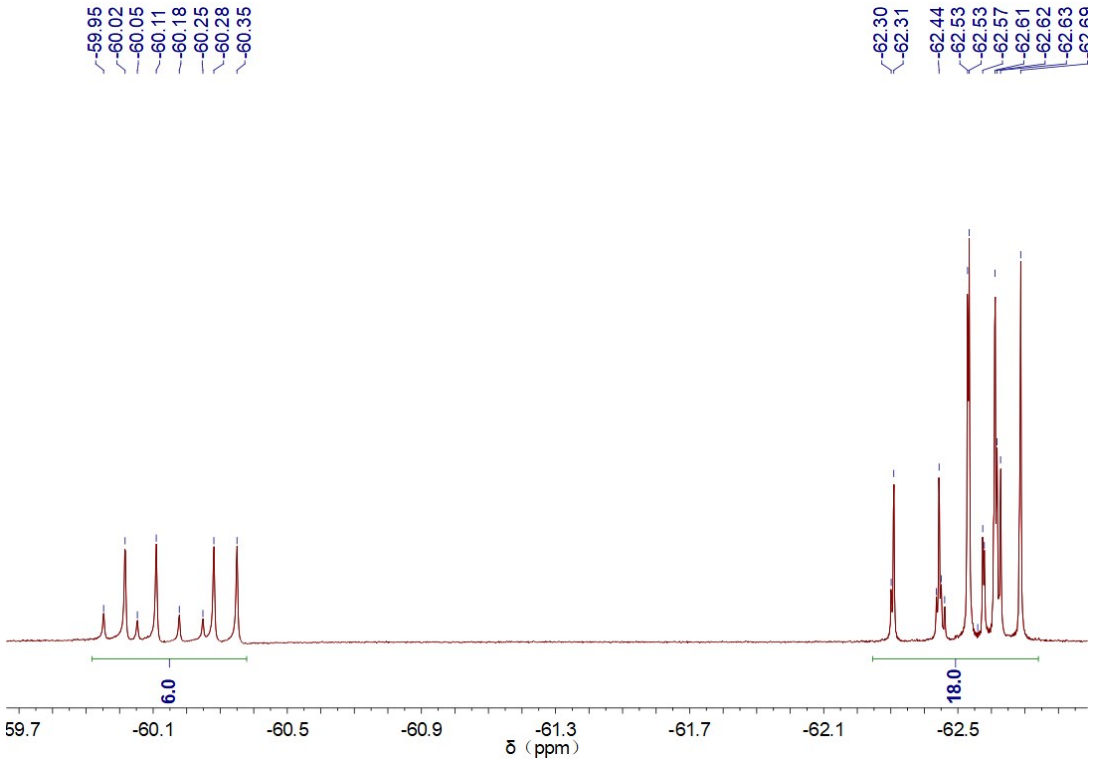

5. High resolution mass spectrometers (HRMS) of all new compounds.

HRMS Spectrum of **btptpH**:

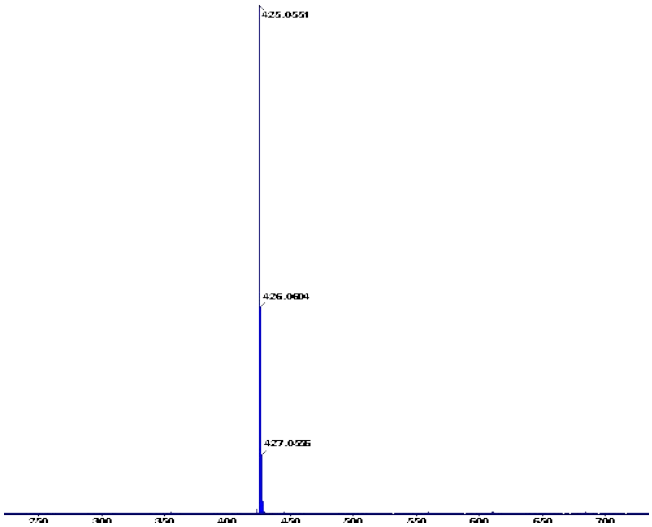

HRMS Spectrum of **Ir1**:

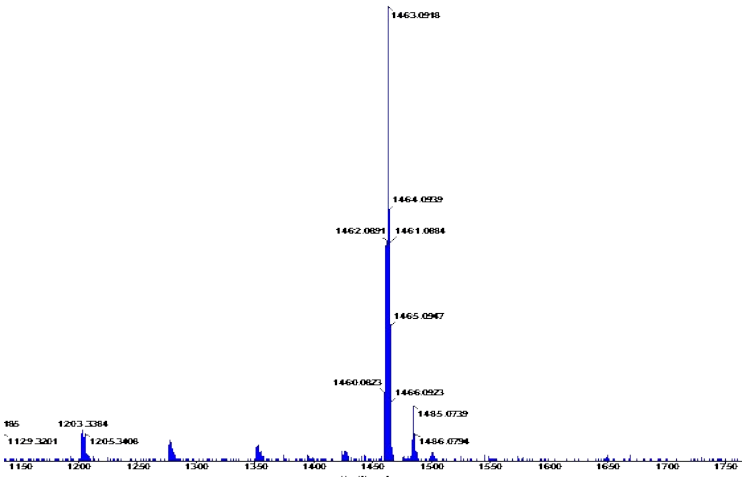

HRMS Spectrum of **Ir2**:

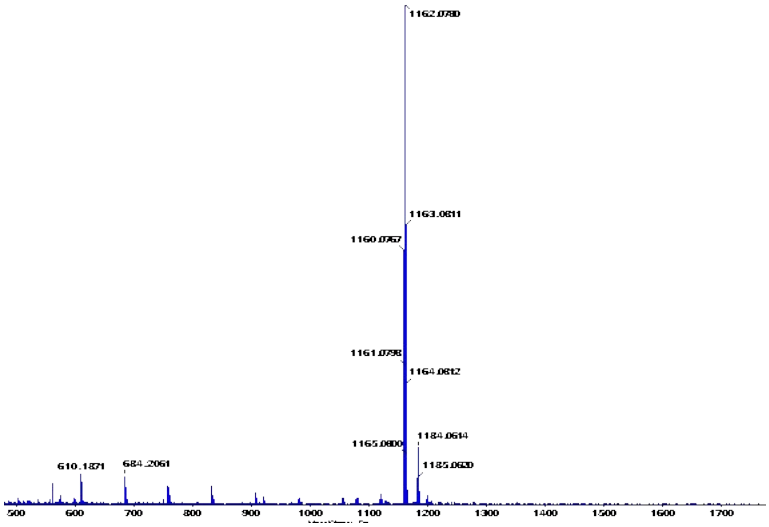

HRMS Spectrum of **qtptpH**:

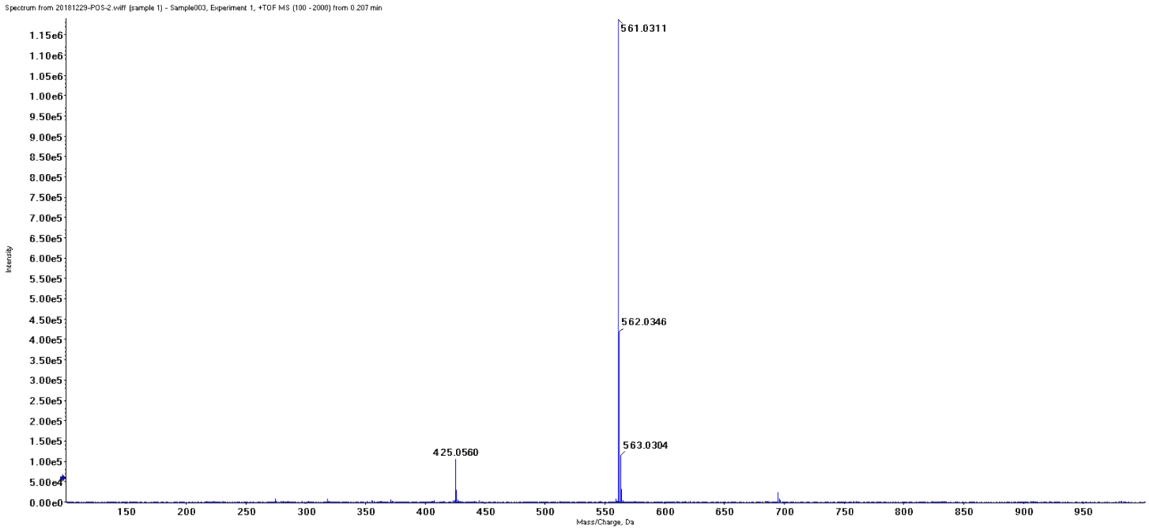

HRMS Spectrum of **Ir3**:

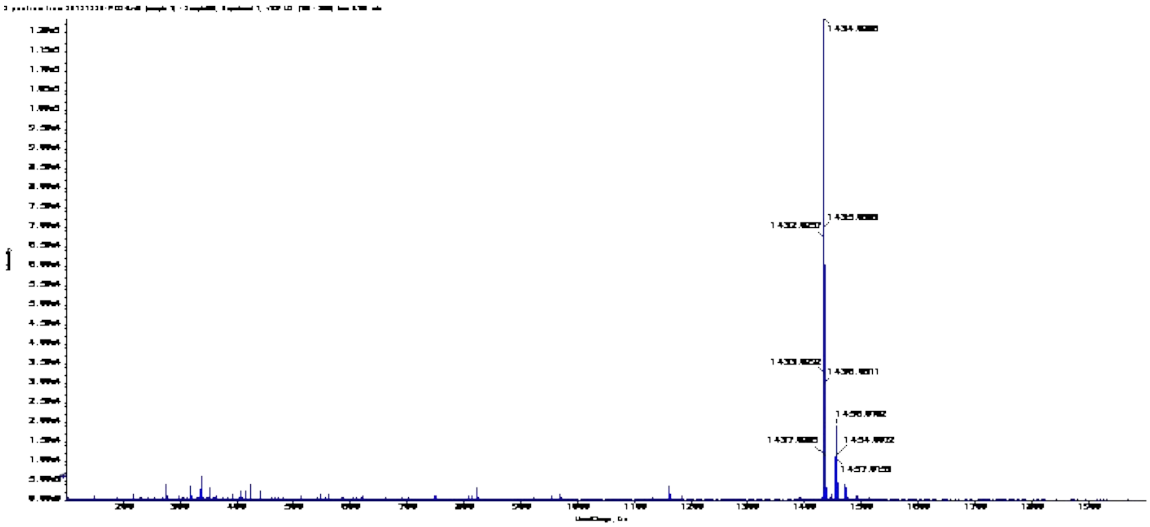

6. References

[1] Becke AD. Density-functional thermochemistry. III. The role of exact exchange, J Chem Phys, 1993; 98: 5648−5652; b) Lee C, Yang W and Parr RG. Development of the Colic-Salvetti correlation-energy formula into a functional of the electron density. Phys Rev B, 1988; 37: 785−789.

[2] Hay PJ and Wadt WRJ. Ab initio effective core potentials for molecular calculations. Potentials for the transition metal atoms Sc to Hg. Chem Phys, 1985; 82: 270−283; b) Wadt WR and Hay PJJ. Ab initio effective core potentials for molecular calculations. Potentials for main group elements Na to Bi. Chem Phys, 1985; 82: 284−298; c) Hay PJ and Wadt WR. Ab initio effective core potentials for molecular calculations. Potentials for K to Au including the outermost core orbitals. J Chem Phys, 1985; 82: 299−310.

[3] Hariharan PC and Pople JA. Accuracy of AH n equilibrium geometries by single determinant molecular orbital theory. Mol Phys, 1974; 27: 209−214.

[4] Lu T and Chen FW. Multiwfn: a multifunctional wavefunction analyzer. J Comput Chem, 2012; 33: 580−592.

[5] Humphrey W, Dalke A and Schulten K. VMD - visual molecular dynamics. J Molec Graphics, 1996; 14: 33−38.

[6] Frisch MJ, Trucks GW, Schlegel HB, Scuseria GE, Robb MA, Cheeseman JR, et al. Gaussian

16, Rev. B.01,Gaussian, Inc., Wallingford CT, 2016.